Published in final edited form as:
Mol Reprod Dev. 2009 April ; 76(4): 321–333. doi:10.1002/mrd.20956.

Permeability of the Rhesus Monkey Oocyte Membrane to Water and Common Cryoprotectants

Jens O.M. Karlsson[1], **Abdelmoneim I. Younis**[2,3], **Anthony W.S. Chan**[3,4], **Kenneth G. Gould**[3], and **Ali Eroglu**[5,*]

[1]Department of Mechanical Engineering, Villanova University, Villanova, Pennsylvania

[2]Department of Obstetrics and Gynecology, Mercer University School of Medicine, Macon, Georgia

[3]Yerkes National Primate Research Center, Atlanta, Georgia

[4]Department of Human Genetics, Emory University School of Medicine, Atlanta, Georgia

[5]Institute of Molecular Medicine and Genetics, Department of Medicine, Medical College of Georgia, Augusta, Georgia

SUMMARY

Successful cryopreservation of oocytes of the rhesus monkey (*Macaca mulatta*) would facilitate the use of this valuable animal model in research on reproduction and development, while providing a stepping stone towards human oocyte cryopreservation and the conservation of endangered primate species. To enable rational design of cryopreservation techniques for rhesus monkey oocytes, we have determined their osmotic and permeability characteristics in the presence of dimethylsulfoxide (DMSO), ethylene glycol (EG), and propylene glycol (PROH), three widely used cryoprotectants. Using nonlinear regression to fit a membrane transport model to measurements of dynamic cell volume changes, we estimated the hydraulic conductivity (L_p) and cryoprotectant permeability (P_s) of mature and immature oocytes at 23.5°C. Mature oocyte membranes were most permeable to PROH (P_s = 0.56 ± 0.05 μm/sec) and least permeable to DMSO (P_s = 0.24 ± 0.02 μm/sec); the permeability to EG was 0.34 ± 0.07 μm/sec. In the absence of penetrating cryoprotectants, mature oocytes had L_p = 0.55 ± 0.05 μm/min/atm, whereas the hydraulic conductivity increased to 1.01 ± 0.10, 0.61 ± 0.07, or 0.86 ± 0.06 μm/min/atm when mature oocytes were exposed to DMSO, EG, or PROH, respectively. The osmotically inactive volume (V_b) in mature oocytes was19.7 ± 2.4% of the isotonic cell volume. The only statistically significant difference between mature and immature oocytes was a larger hydraulic conductivity in immature oocytes that were exposed to DMSO. The biophysical parameters measured in this study were used to demonstrate the design of cryoprotectant loading and dilution protocols by computer-aided optimization.

*Corresponding author: Institute of Molecular Medicine and Genetics, Medical College of Georgia, 1120 15th Street, CB-2803, Augusta, GA 30912. aeroglu@mcg.edu.

INTRODUCTION

Successful cryopreservation of nonhuman primate oocytes would greatly facilitate research on early development, assisted reproduction, and conservation of endangered primate species. Moreover, a successful cryopreservation method that has been developed and thoroughly tested using nonhuman primate oocytes would represent a major stepping-stone towards reliable long-term preservation of human oocytes. Potential benefits of human oocyte cryopreservation include treatment of female infertility when facing cancer and extirpative therapy, as well as avoidance of the many legal and ethical issues associated with embryo freezing.

The first successful cryopreservation of mammalian oocytes was achieved in the 1970s (Parkening et al., 1976; Whittingham, 1977). By the mid-1980s, successful cryopreservation of human oocytes was reported (Chen, 1986). However, it would be a decade until similar success was replicated in other laboratories, due to an incomplete understanding of the mechanisms of oocyte injury associated with freeze-thaw process. These injury mechanisms and their consequences include intracellular ice formation (Leibo et al., 1978), cell lysis (Ashwood-Smith et al., 1988), disruption of cytoskeleton and spindle microtubules (Vincent and Johnson, 1992; Eroglu et al., 1998), premature exocytosis of cortical granules and zona hardening (Carroll et al., 1990), parthenogenetic activation (Shaw and Trounson, 1989; Van der Elst et al., 1992), and polyploidy (Al-Hasani et al., 1987; Eroglu et al., 1998). The findings of several studies indicate that the sensitivity of mammalian oocytes to different cryopreservation-induced injury mechanisms differ among the species. For example, porcine and bovine oocytes are particularly sensitive to chilling injury, while mouse oocytes can better tolerate this mode of cell damage. Furthermore, mouse oocytes exhibit superior recovery from cooling-induced spindle injuries in contrast to primate oocytes (Eroglu et al., 1998; Songsasen et al., 2002b). In recent years, the use of intracytoplasmic sperm injection in conjunction with human oocyte cryopreservation have overcome some of the aforementioned difficulties, and encouraging results have been reported using both slow cooling and vitrification protocols (Porcu et al., 1997; Tucker et al., 1998; Kuleshova et al., 1999; Yoon et al., 2000; Quintans et al., 2002; Fosas et al., 2003; Kuwayama et al., 2005; Boldt et al., 2006; Borini et al., 2006). Despite these promising developments, further research is needed to achieve clinically reliable and robust oocyte cryopreservation techniques.

It has already been shown that optimal cryopreservation protocols can be designed via a rational approach, by predicting the cellular response using mechanistic theoretical models that incorporate cell-specific biophysical parameters such as the plasma membrane permeability and the intracellular ice nucleation coefficients (Mazur et al., 1984; Karlsson et al., 1996). Several studies have been carried out to determine the value of various parameters required by such theoretical models. So far, the membrane permeability to water and cryoprotectant additives (CPAs), as well as ice nucleation coefficients, have been published for mouse (Jackowski et al., 1980; Leibo, 1980; Karlsson et al., 1996; Paynter et al., 1997), rat (Agca et al., 2000), goat (Legal et al., 1994), hamster (Benson and Critser, 1994), cattle (Ruffing et al., 1993; Agca et al., 1998), and human oocytes (Hunter et al., 1992; McGrath et al., 1995; Newton et al., 1999; Paynter et al., 2001) in the presence and

absence of different CPAs. However, similar studies on nonhuman primate oocytes have been limited, due largely to associated high costs. We are only aware of two prior publications of biophysical parameters relevant to cryopreservation of monkey oocytes. The first of these studies reports the water permeability parameters of the plasma membrane and the intracellular ice nucleation coefficients for cynomolgus monkey (*Macaca fascicularis*) oocytes in the absence of CPAs (Younis et al., 1996). The second study has determined the permeability of rhesus monkey (*Macaca mulatta*) oocytes to three CPAs (i.e., glycerol, ethylene glycol [EG], and dimethylsulfoxide [DMSO]) at 30°C and found that rhesus oocytes are less permeable to glycerol than DMSO and EG (Songsasen et al., 2002a). To date, there are no available data on the permeability of rhesus oocytes to propylene glycol (PROH), which is a preferred CPA for cryopreservation of human oocytes (Leibo, 2004).

The objective of the present study was to extend the finding of previous studies by determining the permeability of rhesus monkey oocytes to water and PROH, towards establishment of an optimal thermodynamic pathway for primate oocyte cryopreservation. In addition, the permeability of rhesus oocytes to EG and DMSO at ambient temperature (23.5°C) were determined. The estimated permeability parameters were then used to predict CPA loading and dilution procedures that would minimize the exposure time to CPA while limiting deleterious cell volume perturbations.

RESULTS

Oocyte Morphology

A total of 57 oocytes were collected from four females; however, 15 germinal vesicle (GV) oocytes were discarded due to their either poor morphology (e.g., intracytoplasmic vesicles, polarized granules) or small size. The remaining 28 mature (metaphase II [M II]) and 14 immature (GV to metaphase I [M I]) oocytes were used in the permeability experiments. A representative micrograph of a morphologically normal mature oocyte in isotonic Hypermedium is shown in Figure 1A. All oocytes were exposed to 0.1 M EDTA in CMRL-1066 medium at 37°C for 10 min to ensure spherical shrinkage (Newton et al., 1999). Despite this effort, 26% of the oocytes still exhibited nonspherical shrinkage during exposure to the hypertonic phosphate buffered saline (PBS) and CPA solutions, and were excluded from volume measurements. In experiments with mature oocytes, four out of seven oocytes exposed to hypertonic PBS shrank spherically and were included in the analysis, while the proportion of oocytes maintaining a spherical shape was five out of six for exposure to DMSO, seven out of seven for EG, and five out of eight for PROH. For immature oocytes, the proportion of spherically shrinking cells was two out of four during exposure to hypertonic PBS, two out of two for DMSO exposure, two out of two for EG, and four out of six for PROH. The variations in these frequencies with meiotic stage and solution type were no larger than would be expected by chance (χ^2 test, $P > 0.05$). A typical response of a spherically shrinking mature oocyte exposed to EGis shown in Figure 1B–D. The volume of this oocyte initially decreased for ~1 min as a result of water loss due to the high osmotic pressure exerted by solutes in the extracellular solution; subsequently, the cell volume increased slowly, returning to its initial size within ~16 min. The observed swelling is due primarily to reentry of water into the cell, a transport process that is driven by the

small osmotic pressure differential caused by diffusion of EG molecules from the extracellular solution into the cytoplasm.

Under isotonic conditions, the average cell volume was $(8.3 \pm 0.2) \times 10^{-13}$ m^3 (n=21) for mature oocytes and $(7.9 \pm 0.2) \times 10^{-13}$ m^3 (n=10) for immature oocytes. The difference in size with meiotic stage was not statistically significant; furthermore, no statistically significant variation of isotonic volume was detected between the four donor animals. The average diameter of the pooled sample comprising all 31 oocytes was 115.8 ± 0.8 μm.

Response to Hypertonic PBS

The kinetics of changes in oocyte volume following exposure to hypertonic PBS are summarized in Figure 2, which shows the average and standard error of the normalized cell volume for each time point at which video images were analyzed. When challenged with a hypertonic solution in the absence of penetrating cryoprotectants, the oocyte volumes decreased until osmotic equilibrium was attained. The mature oocytes contracted to ~36% of their original isotonic volume within 2 min and remained shrunken during the remainder of the exposure period. In contrast, the immature oocytes attained equilibrium within 1.5 min, shrinking to ~44% of the initial isotonic volume. The water transport model (Eqs. 1 and 2) was fit to the experimental volume data to obtain estimates of the unknown parameters L_p and V_b for each individual hypertonic exposure experiment. The resulting best-fit values of V_b for mature and immature oocytes were 19.7 ± 2.4% and 28.8 ± 3.6% of the corresponding isotonic cell volumes, respectively. Although the average value of V_b appeared to be somewhat larger in immature oocytes than in M II oocytes, this difference was not statistically significant at the small sample size presently available. The average values of the best-fit hydraulic conductivity are summarized in Table 1. The responses of mature and immature oocytes following exposure to hypertonic saline were simulated using the average values of the hydraulic conductivity and osmotically inactive volume fraction, and are shown in Figure 2. Comparison of the predicted and measured volume changes reveals good agreement between simulations and experiments, which indicates that the use of averaged parameter values in the model yields results that are reasonably representative of the average oocyte response.

Response to Permeant Cryoprotectants

In contrast to the monotonic volume reduction observed following exposure to hypertonic PBS, the initial volume decrease observed when oocytes were exposed to media containing a permeant cryoprotectant was followed by a slow increase in cell volume, with a final equilibrium approximately equal to the isotonic volume (see Fig. 1B–D). Our quantitative analysis of the observed volume changes is summarized in Figure 3, which shows the average of the normalized cell volumes for each time point at which videos were sampled. The classic shrink-swell response evident in Figure 3 is indicative of a cell membrane that is less permeable to the cryoprotectant than to water. For mature oocytes exposed to DMSO, EG, and PROH, the cell volume reached a minimum within 1.00 ± 0.06 min, 0.95 ± 0.05 min and 0.82 ± 0.05 min, respectively. The corresponding volume minima represented a reduction of the initial cell volume by 43 ± 2%, 31 ± 4% and 25 ± 2% for DMSO, EG and PROH, respectively. The equilibration time for cryoprotectant loading was estimated by

determining the time required for the cell to re-swell to at least 95% of the initial volume. In the experiments with mature oocytes, the equilibration time was 11 ± 1, 12 ± 1, and 6 ± 1 min, for DMSO, EG and PROH, respectively. One of the mature oocytes exposed to DMSO exhibited an initial volume reduction in excess of 50%, and an equilibration time less than 6 min; this oocyte was considered to be an outlier and was excluded from calculations. The initial cell volume reduction for immature oocytes was 49 ± 2%, 47 ± 1%, and 29 ± 3% for DMSO, EG and PROH, respectively, that is, somewhat larger than the corresponding volume excursions observed for mature oocytes. The volume minima in experiments with immature oocytes occurred after 0.59 ± 0.09, 0.92 ± 0.08, and 0.96 ± 0.15 min of exposure to DMSO, EG and PROH, respectively, while the corresponding equilibration times were 12 ± 2 min for DMSO, 13 ± 1 min for EG and 9 ± 2 min for PROH. Thus, the main differences between the responses of immature and mature oocytes were a faster initial volume reduction for immature oocytes exposed to DMSO, a significantly larger volume excursion in immature oocytes exposed to EG, and a slower rate of re-expansion in immature oocytes exposed to PROH. Comparing the effects of the different cryoprotectants on oocytes of all meiotic stages, the initial volume reduction was largest during exposure to DMSO, and smallest during exposure to PROH; PROH also had the fastest equilibration time, whereas the uptake of DMSO and EG exhibited comparable kinetics.

Estimation of Membrane Permeability Parameters

To estimate the membrane permeability to permeant cryoprotectants, as well as the effect of these additives on the hydraulic conductivity, the coupled transport model (Eqs. 1–3) was fit to normalized volume data from individual oocytes that had been exposed to solutions containing either DMSO,EG, or PROH. The value of V_b for a given oocyte was determined by multiplying the initial cell volume by the mean osmotically inactive volume fraction reported above for exposure to hypertonic PBS. Thus, the nonlinear regression yielded estimates for the unknown parameters L_p and P_s corresponding to each experiment. The resulting best-fit parameter values were then averaged for each combination of meiotic status and extracellular solution, and are summarized in Table 1. A statistically significant interaction between the effects of solution type and developmental stage on hydraulic conductivity was detected (ANOVA, $P < 0.05$), and pairwise comparisons revealed that the value of L_p in immature oocytes in the presence of DMSO was significantly larger than the hydraulic conductivity in all other experimental groups ($P < 0.05$). The hydraulic conductivity in mature oocytes exposed to DMSO was significantly larger than the value of L_p in mature oocytes exposed to hypertonic PBS or EG ($P < 0.05$), but not PROH. The main effects of solution composition and meiotic status on cryoprotectant permeability were both statistically significant (ANOVA, $P < 0.05$), whereas no significant interaction between the two factors was detected. The main effects appeared to be predominantly a result of the high permeability of mature oocytes to PROH.

The averaged permeability parameters from Table 1 were used to simulate the response of a representative immature or mature oocyte following exposure to each of the three cryoprotectants. The resulting predictions of shrink-swell kinetics for each case are shown in Figure 3. The match between simulation results and the averaged volume measurements is reasonable, especially for experiments with mature oocytes (which had larger sample sizes

than did experiments with immature oocytes). With satisfactory agreement between predictions and experimental data, we proceeded to use our theoretical model to analyze and optimize protocols for addition and dilution of permeant cryoprotectants.

Sensitivity to Osmotic Shock

We adapted viability data reported by Songsasen et al. (2002a) to estimate the sensitivity of oocytes to osmotic shock. Songsasen et al. (2002a) determined the membrane integrity of rhesus oocytes that had been exposed to solutions containing EG in concentrations ranging from 0.1 to 5.0 M for 5 or 10 min, and which were subsequently diluted by a single-step addition of isotonic medium. We used our mathematical model of coupled water- and CPA-transport to simulate the response of oocytes to the addition and dilution of EG during these experiments, yielding predictions of the maximal volume excursion for each solution concentration and equilibration time. For consistency, we used the oocyte permeability parameters and other biophysical properties reported by Songsasen et al. (2002a) when simulating the osmotic sensitivity experiments. In Figure 4, the oocyte viability data from Songsasen et al. (2002a) are correlated with predictions of the maximum volume reduction during cryoprotectant addition, and with the predicted maximum volume increase during the subsequent cryoprotectant removal. Our simulations demonstrated that in the 5-min equilibration experiments, the maximum volume excursion corresponded to the volume minimum of the shrink-swell response during cryoprotectant addition, whereas in the 10-min equilibration experiments, the maximum volume excursion corresponded to the peak volume increase during cryoprotectant dilution. The data in Figure 4 indicate that rhesus monkey oocytes can tolerate volume excursions less than a critical value of ~50%. However, considering that the permeability parameters used to generate the volume excursion predictions in Figure 4 were estimated based on data from only three oocytes (Songsasen et al., 2002a), we felt it prudent to employ a conservative margin of safety in design of procedures for cryoprotectant addition and removal. Thus, loading and dilution protocols were optimized subject to the constraint that all cell volume excursions be smaller than 25% of the isotonic oocyte volume.

Optimization of Cryoprotectant Addition and Removal Protocols

To demonstrate the utility of mathematical models in the design of protocols for oocyte cryopreservation, we used computer simulations to optimize two-step procedures for cryoprotectant addition and removal. We present illustrative results of the optimization of protocols for loading and removal of 1.5 M PROH in mature rhesus monkey oocytes. The objective of the optimization was to minimize the equilibration time (thus reducing potential cytotoxicity), which we have defined as the time required for the volume of intracellular CPA to reach 95% of the equilibrium CPA content during loading, or the time required to remove 95% of the initial intracellular CPA volume during dilution. Furthermore, as explained above, the cell volume was required to remain between 75% and 125% of the isotonic volume, to reduce the risk of damage due to osmotic shock.

The predicted oocyte response during a non optimized single-step exposure to 1.5 M PROH is shown in Figure 5. Although the nonoptimized protocol achieves an equilibration time of ~11 min, the oocytes experience a potentially deleterious volume reduction of 33%. It is also

evident from Figure 5A that this procedure results in oocytes being exposed both intracellularly and extracellularly to relatively high CPA concentrations (≥ 1.4 M) for a duration of ~10 min. Using a simplex algorithm to design a two-step CPA addition procedure, the optimal procedure was determined to consist of an initial 1.87-min exposure to a 1.04 M PROH solution before transfer to 1.5 M PROH. As shown in Figure 5, this loading sequence allows the cell volume excursions to remain below the required 25% limit, while achieving an equilibration time comparable to that obtained with single-step loading (~ 11 min). Moreover, the total CPA dose (exposure time and concentration) is lower in the optimized two-step procedure than in the nonoptimized single-step procedure. For example, the time period during which the intracellular concentration of PROH remains below 1.4 M is more than twice as long in the two-step protocol than in the one-step protocol.

Predictions of cell volume changes and intracellular CPA concentration during removal of CPA from oocytes initially loaded with 1.5 M PROH are shown in Figure 6. For a non optimized single-step dilution process, in which oocytes were exposed directly to isotonic medium or saline, the equilibration time was 1.6 min, but oocytes experienced a volume expansion to 148% of their initial size. For a two-step dilution sequence, the optimal combination of exposure time and PROH concentration for the first dilution solution was determined to be 6.49 min and 0.597 M, respectively. As shown in Figure 6, this dilution protocol successfully maintains the maximum cell volume excursions at or below the specified upper bound of 25%. However, the resulting equilibration time was 7.6 min, that is, almost five times longer than the equilibration time for the single-step dilution process. Nonetheless, this is the fastest possible dilution time if the cell volume is not allowed to exceed 125%, and if the protocol is restricted to a two-step sequence in which the only permitted additive is PROH.

To further improve the dilution process, we allowed the optimization algorithm to consider sucrose in addition to PROH as a possible extracellular additive. Thus, in our second optimization attempt, there were three adjustable process parameters: the concentrations of PROH and sucrose in the first dilution medium, as well as the time of exposure before transfer to isotonic medium. This approach resulted in a two-step protocol with a predicted equilibration time of 1.3 min, that is, even faster than the non optimized single-step dilution procedure. Moreover, as shown in Figure 6, the oocyte volume excursions associated with the optimized protocol do not exceed the imposed bounds of ±25%. The optimized dilution sequence used an initial 32-sec exposure to a solution that contained 1.08Msucrose but no PROH, followed immediately by transfer to an isotonic medium. It should be noted that this particular combination of parameters did not constitute a true global optimum, but represented one possible solution from a family of near-optimal protocols that produced almost identical values of the cost function. For example, a dilution medium containing 0.74 M sucrose (and no PROH), when used with a 57-sec exposure time, resulted in an equilibration time that was only 0.4 sec (0.5%) longer than the equilibration time shown in Figure 6. Each of these near-optimal dilution protocols omitted PROH altogether, but used high sucrose concentrations; to prevent excessive cell shrinkage, the prescribed exposure time decreased as the sucrose concentration increased. Specifically, we identified a family of two-step dilution protocols using solutions containing 0.55–2.5 M sucrose, none of which required more than 1.5 min for equilibration. These near-optimal protocols were

characerized by rapid oocyte shrinkage (to the minimum tolerable cell volume) during exposure to the sucrose solution, which promoted the efflux of PROH by increasing its intracellular concentration. Because the cost function varied only slightly in the vicinity of the optimum, convergence of the optimization algorithm was slow; therefore we terminated the search process before the global optimum was located.

DISCUSSION

We have obtained estimates of the permeability of mature and immature rhesus monkey oocytes to water and three widely used CPAs. Oocytes of nonhuman primates represent a valuable and scarce resource, as a result of which cryobiological investigations in these species are rare, and have typically been limited to small sample sizes. Thus, by contributing additional data to the literature, our findings complement those reported by Songsasen et al. (2002a), which is to our knowledge the only previous investigation of permeability characteristics of rhesus monkey oocytes. For example, the previously published estimates of permeability characteristics during exposure to DMSO were based on observations of three immature and two mature oocytes (Songsasen et al., 2002a), whereas we report permeability measurements based on data from two additional immature oocytes and four additional mature oocytes. Similarly, published estimates of rhesus oocyte membrane permeability in the presence of EG were based on measurements on four immature and three mature cells (Songsasen et al., 2002a), to which we have added data from two immature and seven mature oocytes. We have also obtained the first measurements of permeability of rhesus monkey oocytes to PROH, as well as the first estimates of hydraulic conductivity in the absence of permeant cryoprotectants. Furthermore, we have incorporated our biophysical parameter measurements into mathematical models that were used to optimize multi-step procedures for addition and removal of CPAs, based on simulations of oocyte response.

The hydraulic conductivity (water permeability) estimated for rhesus monkey oocytes in the absence of permeant cryoprotectants was lower than the best-fit values of L_p obtained in oocytes exposed to DMSO and EG (and in mature oocytes, also PROH); the increase in L_p in the presence of DMSO was statistically significant. In contrast, Rule et al. (1980) showed that the presence of DMSO causes a reduction of the estimated value of the hydraulic conductivity for fibroblasts, an effect opposite to that observed in the present study. Moreover, Van den Abbeel et al. (2007) found that the hydraulic conductivity of human oocytes decreased in the presence of DMSO and EG. However, several other studies have reported an apparent increase in the hydraulic conductivity of oocytes in the presence of DMSO (McGrath et al., 1992; Marlow et al., 1994; Paynter et al., 1999) as well as PROH (Fuller et al., 1992; Van den Abbeel et al., 2007), which is consistent with our present findings.

In our room-temperature experiments, the hydraulic conductivity of rhesus monkey oocytes at all developmental stages was largest in the presence of DMSO. Moreover, the difference between the mean values of L_p in the presence of DMSO and EG was statistically significant. These trends differ from previously published observations at a higher temperature: at 30°C, the hydraulic conductivity was reported to be of approximately the same magnitude (~1 μm/min/atm) in the presence of either DMSO or EG, the former

cryoprotectant being associated with somewhat smaller water permeability (Songsasen et al., 2002a). Because permeability coefficients are governed by the Arrhenius relationship, the lower temperature in the present study is expected to result in smaller values of L_p. Our L_p estimate for mature oocytes exposed to EGis approximately half the corresponding value reported at 30°C (Songsasen et al., 2002a), suggesting an activation energy of ~7×10^4 J/mol. However, for immature rhesus monkey oocytes exposed to DMSO, our room-temperature value of L_p is larger than the value obtained by Songsasen et al. (2002a) at 30°C, which requires a physically implausible negative activation energy. Moreover, for mature rhesus monkey oocytes exposed to DMSO as well as immature oocytes exposed to EG, L_p at 23.5°C was only 6–7%smaller than the corresponding value of L_p reported for experiments by Songsasen et al. (2002a) at 30°C; for these observations to be consistent with each other, the activation energy associated with the hydraulic conductivity would have to be improbably small (<10^4 J/mol). In comparison, the hydraulic conductivity of mature human oocytes has been reported to have an activation energy of 4.7×10^4 J/mol (Van den Abbeel et al., 2007) or 6.0×10^4 J/mol (Mullen et al., 2008) in the presence of EG, and 6.2×10^4 J/mol in the presence of DMSO (Paynter et al., 1999).

There are several possible sources for the apparent inconsistencies between our measurements of hydraulic conductivity and those reported by Songsasen et al. (2002a). First, the total number of rhesus oocytes was, by necessity, relatively small in both studies (n=2–7 in the present study, and n=2–4 in the work by Songsasen et al., 2002a), leading to uncertainty in the values of the permeability coefficients. In addition, in the present study, oocyte volumes were analyzed at 10-sec intervals or shorter during the first 2 min of each experiment, whereas Songsasen et al. (2002a) obtained less frequent volume measurements. Because the value of L_p estimated by curve-fitting techniques is expected to be most sensitive to the initial phase of the shrink-swell response (during which water leaves the cell due to osmotic forces), the accuracy of the parameter estimate will be affected by the number of data points acquired during oocyte shrinkage. On the average, we obtained volume measurements at ~10 timepoints during the shrinkage phase, whereas Songsasen et al. (2002a) collected only 1–3 data points during this critical interval. Because of the higher sampling rate in the present study, as well as the larger number of mature oocytes used in permeability measurement experiments, we expect the corresponding parameter estimates to be somewhat more reliable than those reported by Songsasen et al. (2002a).

The present estimate for the room-temperature permeability of immature oocytes to EG was slightly smaller than the value of 0.18 μm/sec obtained by Songsasen et al. (2002a) for immature rhesus monkey oocytes at 30°C, which is consistent with an Arrhenius-type temperature-dependence of P_s. On the other hand, Songsasen et al. (2002a) reported an EG permeability of 0.14 μm/sec for mature rhesus oocytes at 30°C, which is less than half of the room-temperature value obtained in the present investigation, and therefore implies a negative activation energy. This anomalous result requires further investigation, but appears to be a result of the fact that the volume excursions for EG reported in the study by Songsasen et al. (2002a) were on the average larger than those observed in the present study. The minimum volume during the shrink-swell response depends on the L_p/P_s ratio, with larger volume excursions being associated with larger values of L_p/P_s. Thus, the larger value of P_s obtained for EG in the present study is consistent with the expected results of curve-

fitting data that have a smaller volume excursion. Due to the small number of cells analyzed for the experimental group in question [n=3 in Songsasen et al. (2002a), and n=7 in the present study], it is difficult to determine whether the apparent difference in the average volume minima (and hence, P_s) is statistically significant. Even though, to the best of our knowledge, there are no additional published studies on the membrane permeability of rhesus monkey oocytes, the room-temperature permeability to EG has recently been measured for mature human oocytes by Van den Abbeel et al. (2007), who obtained P_s=0.20 μm/sec at 22°C, as well as by Mullen et al. (2008), who obtained P_s=0.15 μm/sec at 25°C. These values are both smaller than our estimate of P_s for EG in mature rhesus monkey oocytes, suggesting that our value may be too large. However, the neither of the two published EG permeability values for human oocytes at room temperature is smaller than the EG permeability reported for mature rhesus monkey oocytes at 30°C, suggesting that the P_s value obtained by Songsasen et al. (2002a) may be an underestimate. Our estimate of EG permeability in immature rhesus monkey oocytes was similar to the value reported for mature human oocytes by Mullen et al. (2008).

The membrane permeability to DMSO estimated for mature rhesus monkey oocytes in the present study was equivalent to measurements of DMSO permeability previously reported for mature human oocytes at room temperature (22–24°C): for example, Paynter et al. (1999) obtained $P_s = 0.25 \pm 0.04$ μm/sec, and Van den Abbeel et al. (2007) obtained $P_s = 0.26 \pm 0.02$ μm/sec. A slightly higher value (0.32 μm/sec) was obtained by Newton et al. (1999) for fresh M II human oocytes, although the same study reported a DMSO permeability of 0.25 μm/sec for M II oocytes that had failed to fertilize. The DMSO permeabilities reported by Songsasen et al. (2002a) for immature and mature rhesus monkey oocytes at 30°C are approximately fourfold larger than the corresponding values obtained in the present study at room temperature. An increase in permeability with temperature is expected due to the known Arrhenius behavior of this parameter, and the magnitude of the difference in permeability at the two temperatures is consistent with an activation energy on the order $\sim 10^5$ J/mol, which is similar to the value 8.7×10^4 J/mol reported for the activation energy of the DMSO permeability in human oocytes (Paynter et al., 1999).

Our estimate of oocyte membrane permeability to PROH represents the first such measurement for a nonhuman primate species. The membrane permeability of human oocytes to PROH has previously been measured using both microperfusion (Paynter et al., 2001; Van den Abbeel et al., 2007) and diffusion chamber techniques (Fuller et al., 1992; Bernard and Fuller, 1996), yielding values in the range 0.28–0.82 μm/sec at room temperature. Although the PROH permeability value that we obtained for mature rhesus monkey oocytes falls in the middle of the range values reported for human oocytes, it is noteworthy that the two studies using microperfusion both yielded estimates that were smaller than our value of P_s, whereas the two studies using diffusion chamber techniques both yielded values that were larger than our permeability estimate. The microperfusion technique is considered to be more accurate than the diffusion chamber technique for estimating oocyte membrane permeability to PROH (Bernard and Fuller, 1996). Thus, if only studies based on microperfusion methods are considered, it appears that the room-temperature permeability to PROH may be larger in mature rhesus monkey oocytes than in human oocytes.

The results of the present investigation indicate that, at room temperature, rhesus monkey oocytes of all meiotic stages were most permeable to PROH, whereas their permeabilities to DMSO and EG were comparable in magnitude. This observation is consistent with the findings of Van den Abbeel et al. (2007), who compared the permeabilities of in vitro matured human oocytes to the same three cryoprotectants at room temperature, and found that the membrane permeability to PROH was 40–80% larger than the permeability to either DMSO, or EG, the latter difference being statistically significant. In contrast, Paynter et al. (1999, 2001) published two separate studies using the same experimental method to determine the permeability of human oocytes to PROH and to DMSO, and found that although the permeability to PROH was slightly larger than to DMSO, the difference was not statistically significant at room temperature. Nonetheless, when these investigators repeated their experiments at a lower temperature (10°C), the permeability to PROH was found to be significantly larger than the DMSO permeability (Paynter et al., 2001). From the perspective of reducing the time required for CPA loading and removal, as well as limiting potential injury due to osmotic shock, the use of PROH as a penetrating CPA for rhesus monkey oocytes would be advantageous based on its higher permeability and smaller volume excursions compared to DMSO or EG. However, the relative cytotoxicity of CPAs, which was not assessed in the present study, must also be taken into account when selecting an optimal additive.

We used computer simulations to evaluate various stepwise protocols for addition and dilution of PROH, enabling simultaneous optimization of the solution compositions and exposure periods using an automated algorithm based on the simplex search technique. Other investigators have used membrane transport models to predict the extracellular solution compositions required to prevent damaging volume changes during CPA loading and removal, but have apparently not systematically varied the exposure times associated with each step (e.g., Arnaud and Pegg, 1990; Newton et al., 1999; Mullen et al., 2008). As a result, previous attempts to use computer simulations to guide the design of multi-step CPA addition and dilution techniques have typically resulted in protocols that are longer in duration than the corresponding single-step methods (e.g., Arnaud and Pegg, 1990; Newton et al., 1999; Mukherjee et al., 2007). In contrast, the present multi-parameter optimization approach allowed us to design two-step CPA addition and removal methods that were as fast as single-step methods, but without the deleterious cell volume excursions associated with the latter.

When we allowed the dilution media to contain an osmotic buffer (sucrose) in addition to salt and CPA, the optimization algorithm prescribed that PROH be omitted from the extracellular solutions and that cells be initially exposed to a high concentration of sucrose for a very short duration. As illustrated in Figure 6, the result of this treatment was to invert the volume excursion profile compared to conventional stepwise dilution sequences: the initial response was a cell volume decrease (as opposed to the initial swelling observed in the absence of sucrose), because the extracellular osmotic buffer was present in sufficiently high concentration to make the chemical potential difference in Equation (2) (and thus, the osmotic pressure difference) negative after ~1 sec. Although osmotic buffers have been used in dilution media since the work of Lovelock (1952), extracellular solutions previously proposed have not omitted the permeating CPA (Lovelock, 1952; Arnaud and Pegg, 1990),

or have not used the osmotic buffer solute in concentrations sufficient to rapidly reverse the sign of the osmotic pressure difference (Ebertz and McGann, 2004; Mukherjee et al., 2007; Mullen et al., 2008). Whereas previous strategies have limited the concentration of impermeant solutes to prevent the equilibrium cell volume from falling below the lower volume excursion limit (e.g., Gilmore et al., 1997; Ebertz and McGann, 2004), our simulations demonstrated that such constraints result in suboptimal protocols; instead, deleterious volume reductions should be avoided by transferring cells out of the osmotic buffer solution well before equilibrium is attained. A similar concept was described by Arnaud and Pegg (1990), who proposed a dilution scheme for platelets loaded with 1 M glycerol, in which cells were initially exposed to a 0.35 M glycerol solution containing impermeant solutes at an osmolality 700 mOsm; cell shrinkage was stopped after 4 min by addition of distilled water. However, an important feature of the sucrose-aided dilution strategy developed in the present work is that the osmotic pressure in the first dilution solution should be sufficiently high to rapidly reduce the cell volume to values smaller than the isotonic volume, with continuing cell shrinkage to the limit of tolerable contraction. The effect of quickly inducing cell shrinkage during the initial dilution step is to squeeze the CPA out of the cell by increasing the intracellular CPA concentration (which increases the driving force for transport across the cell membrane). In contrast, the use of osmotic buffers in previous studies has predominantly been for the purpose of limiting the amount of cell swelling (i.e., preventing the cell volume from increasing above a prescribed upper bound).We are unaware of prior CPA removal procedures based on the application of high osmotic pressure to squeeze out intracellular CPA, and believe this strategy has the potential yield to improved cell viability by reducing the total time required for dilution.

In summary, we have determined the permeability of rhesus monkey oocyte membranes to three common penetrating CPAs, including the first published estimates of the permeability to PROH. We have also reported the first measurements of the baseline hydraulic conductivity of these cells in the absence of permeant solutes. Furthermore, we have demonstrated the value of such fundamental biophysical parameter measurements by designing optimal protocols for loading and removal of PROH based on computer simulations of the oocytes' osmotic response. Adapting the simplex optimization algorithm to this task, we were able to simultaneously tune multiple process parameters, including the concentrations of permeant and impermeant solutes in the extracellular solutions, as well as the exposure time to each solution (a variable that has previously not received much attention). This approach is based on a well-defined optimization objective (minimization of the equilibration time, subject to cell volume excursion limits), and eschews unnecessary design constraints that have confounded other optimization studies. As a result, our algorithm generated predictions that allowed us to identify a novel strategy for dilution of permeant CPAs using osmotic buffers such as sucrose. The findings of the present study contribute to the modest knowledge base of primate oocyte cryobiology, and serve as a starting point for the rational design of cryopreservation protocols for these valuable cells.

MATERIALS AND METHODS

Chemicals

All chemicals were purchased from Sigma (St. Louis, MO) unless otherwise stated.

Ovarian Stimulation and Retrieval of Oocytes

All protocols involving rhesus monkeys (*M. mulatta*) were reviewed and approved by the Institutional Animal Care and Use Committees at Yerkes National Primate Research Center and Medical College of Georgia. Adult rhesus females were individually caged and housed at Yerkes National Primate Research Center in rooms with a constant temperature of 23°C and controlled light cycle (12 hr light:12 hr dark). To induce growth of multiple follicles, rhesus females exhibiting regular menstrual cycles were given twice daily intramuscular injections of 30 IU of recombinant human follicle stimulating hormone (rhFSH; Follistim, Organon, Inc., Roseland, NJ) for 8–10 days beginning on Day 1–3 of their menstrual cycle. From day 7 on, human recombinant luteinizing hormone (rhLH; 60 IU/day, Luveris, Organon) and a gonadotropin releasing hormone (GnRH) antagonist (Antagon, 5 μg/kg subcutaneous, Organon) were given twice and once daily, respectively. To monitor the follicle growth, ultrasonography was performed on day 7 and on subsequent days of the stimulation. When at least five follicles reached a diameter ≥ 3 mm, the stimulation was stopped and a single intramuscular injection of 1,000 IU of human chorionic gonadotropin (hCG; Serono Laboratories, Norwell, MA) was administered to induce meiotic maturation. Twenty-seven to thirty hours after hCG injection, rhesus females were anaesthetized with ketamine hydrochloride and maintained on a mixture of isoflurone/oxygen while follicle contents were laparoscopically aspirated into several collection tubes containing 2 ml warm HEPES-buffered human tubal fluid (HTF) medium (SAGE BioPharma, San Clemente, CA) with 20 IU/ml heparin. Next, cumulus–oocyte complexes (COCs) were recovered from the aspirates using a stereomicroscope, and transported in HEPES-HTF at 37°C from Yerkes National Primate Research Center to the Medical College of Georgia in a portable incubator (~2.5 hr drive). Immediately upon arrival, the COCs were first treated with hyaluronidase (120 IU/ml) for 3–4 min, and then pipetted up and down to remove cumulus cells. Subsequently, cumulus-free oocytes were washed twice in modified CMRL-1066 medium containing 0.2 mM sodium pyruvate, 1 mM glutamine, 10 mM sodium lactate, and 10% fetal bovine serum (FBS). Before use, drops of modified CMRL-1066 were overlaid with embryo-tested mineral oil and equilibrated overnight under a humidified atmosphere of 5% CO_2 in air. The M II oocytes were cultured in modified CMRL-1066 for at least 1 hr, and then used in experiments. Oocytes at other meiotic stages—that is, GV, GV breakdown (GVBD), and M I–were considered as immature and cultured in modified CMRL-1066 medium for up to 16 hr to allow sufficient time for maturation before use in experiments. During this extended culture period, the oocytes were frequently examined, and the ones that progressed to the MII stage were then used in experiments without further time in culture.

Permeability Measurements

All permeability experiments were conducted at room temperature, which was 23.5°C. The initial conditions for all experiments were established by exposure of oocytes to Hypermedium (Eroglu et al., 2003) at isotonic osmolality (288 mOsm). To determine the

water permeability in the absence of cryoprotectants, we prepared a hypertonic solution (1,339 mOsm) of PBS from 10-fold concentrated stock (HyClone, Logan, UT). Osmolalities were measured using a freezing point osmometer (Micro-Osmette, Precision Systems, Inc., Natick, MA). One-molar solutions of three CPAs were prepared by dilution with isotonic Hypermedium. Based on density values available in the literature, the final concentrations of PROH, DMSO, and EG were calculated to be 1.0, 1.1, and 1.1 M, respectively. Sudden exposure of oocytes to a CPA solution or hypertonic PBS was performed using an approach similar to that published by Edashige et al. (2003). Briefly, a 60-mm dish containing an 80-μl drop of isotonic Hypermedium and a 160-μl drop of anisotonic solution (hypertonic PBS or one of the CPA solutions) was prepared under a laminar flow hood. The drops were placed close to each other and covered with mineral oil before placing the dish on the stage of an inverted microscope (Axiovert 135, Zeiss, Thornwood, NY) with Hoffman modulation optics. First, a cumulus-free oocyte was transferred to the 80-μl drop of the isotonic Hypermedium, and immobilized at the tip of a holding pipette by applying negative pressure using a micromanipulation system (Narishige, East Meadow, NY); an image of the oocyte in the isotonic Hypermedium was recorded at this time to establish the initial cell size. Next, the tip of the holding pipette with the immobilized oocyte was inserted into a small volume (less than 0.5 μl) of isotonic Hypermedium within the tip portion of a second, outer pipette that had an inner diameter slightly larger than a typical rhesus oocytes (see Fig. 1A). The whole system (holding pipette-oocyte-outer pipette) was moved from the 80-μl drop of isotonic Hypermedium to the 160-μl drop containing either the hypertonic PBS or one of the CPA solutions. Finally, the oocyte was suddenly exposed to the anisotonic solution by quickly pulling the holding pipette from inside the outer pipette, and then immediately removing the outer pipette from the drop. The oocyte remained attached to the tip of the holding pipette during the entire exposure time. Volumetric responses of oocytes to the anisotonic solutions were recorded using a CCD camera (DXC-107A, Sony Corporation, Tokyo, Japan) mounted on the microscope, the analog video output of which was continuously digitized using a DVD recorder (DMR-E80H, Panasonic, Secaucus, NJ). The resulting digital videos were transferred to a personal computer, and oocyte images were extracted for analysis by sampling the video recordings at intervals of 10 sec or shorter during the first 2 min of exposure to the anisotonic solution, and subsequently at 2-min intervals or shorter. The public domain software NIH Image (National Institutes of Health, Bethesda, MD) was used for morphometry. The oocyte volume at each time point was calculated from the projected cross-sectional areas (Leibo, 1980); only oocytes remaining spherical in shape throughout shrinkage and/or re-expansion were included in data analysis.

Theoretical Model

The transient changes in cell volume following exposure to solutions of cryoprotectant or hypertonic saline were modeled using a coupled mass-transport model defined by the following equations:

$$V = V_w + V_s + V_i + V_b \quad (1)$$

$$\frac{dV_w}{dt} = \frac{L_p A}{\bar{v}_w}(\mu_w^{ex} - \mu_w^{in}) \quad (2)$$

$$\frac{dV_s}{dt} = P_s \bar{v}_s A(c_s^{ex} - c_s^{in}) \quad (3)$$

where V and A are the cell volume and surface area, respectively; V_w, V_s, V_i, the intracellular volumes of water, permeant solute and impermeant solute, respectively; V_b, the osmotically inactive volume; $\bar{v}_w$, $\bar{v}_s$, the partial molar volume of water and permeant solute, respectively; μ_w^{in}, μ_w^{ex}, the chemical potentials of intracellular and extracellular water, respectively; c_s^{in}, c_s^{ex}, the concentrations of permeant solute in the intracellular and extracellular compartments, respectively; t, time elapsed since exposure to the anisosmotic solution; L_p, hydraulic conductivity of the cell membrane; P_s, membrane permeability to the permeant solute. The magnitude of the water chemical potential was estimated using the approximation:

$$\mu_w \approx \mu_w^0(T) + \Re T \ln x_w \quad (4)$$

where μ_w^0 is the chemical potential of pure water; T, absolute temperature; $\Re$, the universal gas constant; x_w, the mole fraction of water (relative to the total number of osmotically active particles in the solution). Computer simulations of the dynamic changes in oocyte volume were performed using custom software developed by one of the authors (JOMK) in the MATLAB® programming language (The MathWorks, Inc., Natick, MA); the system of nonlinear differential equations (Eqs. 2 and 3) was numerically integrated using a modified second-order Rosenbrock solver as implemented in MATLAB®.

Data Analysis

Data are reported as average values with error bars representing the standard error of the mean (SEM). Whereas oocyte volume measurements are presented in aggregated form for clarity (i.e., mean and SEM at each timepoint), the coupled mass-transport model was fit to transient volume data for every oocyte individually, to estimate the osmotically inactive volume (V_b) or permeability parameters (L_p and P_s) for each cell. The nonlinear curve fitting method used the Nelder–Mead simplex algorithm to find the combination of parameter values that minimized the mean of the squares of the residues, and was implemented in MATLAB® software developed by one of the authors (JOMK). The proportions of isotropically shrinking cells in each experimental group were compared by χ^2 analysis. Values of V_b and the osmotically inactive volume fraction (i.e., V_b divided by the isotonic cell volume) for mature and immature cells were compared using Student's *t*-test. Two-way analysis of variance (ANOVA) was used to evaluate the effects of donor animal and meiotic stage on isotonic cell volume, as well as the effects of extracellular solution and meiotic status on the best-fit permeability parameters L_p and P_s. Post-hoc comparisons were performed using the Tukey honestly significant difference (HSD) test. Effects were considered statistically significant when the *P*-value was less than 0.05.

Optimization of Cryoprotectant Addition and Dilution

Computer simulations of oocyte response during exposure to various extracellular solutions were used to optimize two-step methods for addition and dilution of a penetrating cryoprotectant. In the present study, we report the optimization of solutions and procedures for loading mature rhesus monkey oocytes with 1.5 M PROH, and for subsequent removal of the CPA from these cells. The two-step addition and dilution procedures consisted of sequential exposure of oocytes to two aqueous solutions; all solutions contained isotonic levels of saline (modeled as 143.4mMNaCl), but had different concentrations of PROH and sucrose. To design a method for CPA loading, the concentration of PROH in the first solution and the time of exposure before transfer to the second solution were variable parameters to be simultaneously optimized; the second solution always contained 1.5 M PROH, and oocytes were held in this solution until equilibrium was reached. We developed CPA dilution techniques both with and without sucrose as an osmotic buffer. Thus, the initial two-step dilution process, which did not use sucrose, was designed by simultaneously optimizing the PROH concentration in the first solution, as well as the time of exposure to this solution; the final step always consisted of equilibration in isotonic saline containing no other additives. Next, we developed an alternative dilution process by allowing the first solution to contain variable amounts of PROH and/or sucrose, and simultaneously optimizing three parameters: the concentration of PROH, the concentration of sucrose, and the time of exposure before transfer to isotonic saline. The Nelder–Mead simplex algorithm was used to systematically search for a combination of parameter values that minimize a specified cost function. For optimization of CPA addition, the cost function was defined as the time required for the intracellular CPA content to reach 95% of the desired equilibrium level. For optimization of CPA dilution, the cost function was defined as the time required to remove 95% of the initial intracellular CPA content. The rationale for minimizing the total equilibration time is to reduce the effects of cryoprotectant toxicity. To prevent injury associated with excessive cell expansion or contraction due to osmotic shock, penalties were added to the cost function whenever the predicted maximum excursion of the oocyte volume exceeded a limit of ±25% relative to the isotonic cell volume. All protocol optimizations were performed using MATLAB® programs written by one of the authors (JOMK).

Acknowledgments

The authors thank Ms. Jill Johnson-Ward and Ms. Marissa Markyna for technical assistance. This study was supported by Grant Number R01HD049537 from the National Institute of Child Health and Human Development awarded to A.E.

REFERENCES

Agca Y, Liu J, Peter AT, Critser ES, Critser JK. Effect of developmental stage on bovine oocyte plasma membrane water and cryoprotectant permeability characteristics. Mol Reprod Dev. 1998; 49:408–415. [PubMed: 9508092]

Agca Y, Liu J, Critser ES, Critser JK. Fundamental cryobiology of rat immature and mature oocytes: Hydraulic conductivity in the presence of Me_2SO, Me_2SO permeability, and their activation energies. J Exp Zool. 2000; 286:523–533. [PubMed: 10684576]

Al-Hasani S, Diedrich K, van der Ven H, Reinecke A, Hartje M, Krebs D. Cryopreservation of human oocytes. Hum Reprod. 1987; 2:695–700. [PubMed: 3437048]

Arnaud FG, Pegg DE. Permeation of glycerol and propane-1,2-diol into human platelets. Cryobiology. 1990; 27:107–118. [PubMed: 2331885]

Ashwood-Smith MJ, Morris GW, Fowler R, Appleton TC, Ashorn R. Physical factors are involved in the destruction of embryos and oocytes during freezing and thawing procedures. Hum Reprod. 1988; 3:795–802. [PubMed: 3220945]

Benson CT, Critser JK. Variation of water permeability (L_p) and its activation-energy (E_a) among unfertilized golden-hamster and Icr murine oocytes. Cryobiology. 1994; 31:215–223. [PubMed: 8050267]

Bernard A, Fuller BJ. Cryopreservation of human oocytes: A review of current problems and perspectives. Hum Reprod Update. 1996; 2:193–207. [PubMed: 9079413]

Boldt J, Tidswell N, Sayers A, Kilani R, Cline D. Human oocyte cryopreservation 5-year experience with a sodium-depleted slow freezing method. Reprod Biomed Online. 2006; 13:96–100. [PubMed: 16820118]

Borini A, Lagalla C, Bonu MA, Bianchi V, Flamigni C, Coticchio G. Cumulative pregnancy rates resulting from the use of fresh and frozen oocytes: 7 years' experience. Reprod Biomed Online. 2006; 12:481–486. [PubMed: 16740222]

Carroll J, Depypere H, Matthews CD. Freeze-thaw-induced changes of the zona pellucida explains decreased rates of fertilization in frozen-thawed mouse oocytes. J Reprod Fertil. 1990; 90:547–553. [PubMed: 2250252]

Chen C. Pregnancy after human oocyte cryopreservation. Lancet. 1986; 1:884–886. [PubMed: 2870356]

Ebertz SL, McGann LE. Cryoprotectant permeability parameters for cells used in a bioengineered human corneal equivalent and applications for cryopreservation. Cryobiology. 2004; 49:169–180. [PubMed: 15351688]

Edashige K, Yamaji Y, Kleinhans FW, Kasai M. Artificial expression of aquaporin-3 improves the survival of mouse oocytes after cryopreservation. Biol Reprod. 2003; 68:87–94. [PubMed: 12493699]

Eroglu A, Toth TL, Toner M. Alterations of the cytoskeleton and polyploidy induced by cryopreservation of metaphase II mouse oocytes. Fertil Steril. 1998; 69:944–957. [PubMed: 9591507]

Eroglu A, Lawitts JA, Toner M, Toth TL. Quantitative microinjection of trehalose into mouse oocytes and zygotes, and its effect on development. Cryobiology. 2003; 46:121–134. [PubMed: 12686202]

Fosas N, Marina F, Torres PJ, Jove I, Martin P, Perez N, Arnedo N, Marina S. The births of five Spanish babies from cryopreserved donated oocytes. Hum Reprod. 2003; 18:1417–1421. [PubMed: 12832365]

Fuller BJ, Hunter JE, Bernard AG, McGrath JJ, Curtis P, Jackson A. The permeability of unfertilised oocytes to 1,2 propanediol—A comparison of mouse and human cells. Cryo-Letters. 1992; 13:287–292.

Gilmore JA, Liu J, Gao DY, Critser JK. Determination of optimal cryoprotectants and procedures for their addition and removal from human spermatozoa. Hum Reprod. 1997; 12:112–118. [PubMed: 9043914]

Hunter J, Bernard A, Fuller B, McGrath J, Shaw RW. Plasma membrane water permeabilities of human oocytes: The temperature dependence of water movement in individual cells. J Cell Physiol. 1992; 150:175–179. [PubMed: 1730781]

Jackowski S, Leibo SP, Mazur P. Glycerol permeabilities of fertilized and unfertilized mouse ova. J Exp Zool. 1980; 212:329–341. [PubMed: 7420045]

Karlsson JOM, Eroglu A, Toth TL, Cravalho EG, Toner M. Fertilization and development of mouse oocytes cryopreserved using a theoretically optimized protocol. Hum Reprod. 1996; 11:1296–1305. [PubMed: 8671443]

Kuleshova L, Gianaroli L, Magli C, Ferraretti A, Trounson A. Birth following vitrification of a small number of human oocytes: Case report. Hum Reprod. 1999; 14:3077–3079. [PubMed: 10601099]

Kuwayama M, Vajta G, Kato O, Leibo SP. Highly efficient vitrification method for cryopreservation of human oocytes. Reprod Biomed Online. 2005; 11:300–308. [PubMed: 16176668]

Legal F, Gasqui P, Renard JP. Differential osmotic behavior of mammalian oocytes before and after maturation—A quantitative-analysis using goat oocytes as a model. Cryobiology. 1994; 31:154–170. [PubMed: 8004996]

Leibo SP. Water permeability and its activation-energy of fertilized and unfertilized mouse ova. J Membr Biol. 1980; 53:179–188. [PubMed: 7190193]

Leibo, SP. Cryopreservation of mammalian oocytes. In: Tulandi, T.; Gosden, R., editors. Preservation of fertility. London: Taylor & Francis; 2004. p. 141-155.

Leibo SP, McGrath JJ, Cravalho EG. Microscopic observation of intracellular ice formation in unfertilized mouse ova as a function of cooling rate. Cryobiology. 1978; 15:257–271. [PubMed: 710156]

Lovelock JE. Resuspension in plasma of human red blood-cells frozen in glycerol. Lancet. 1952; 1:1238–1239. [PubMed: 14939773]

Marlow, DC.; McGrath, JJ.; Sauer, HJ.; Fuller, BJ. Advances in heat and mass transfer in biological systems. New York: ASME Press; 1994. Permeability of frozen and non-frozen mouse oocytes to dimethylsulphoxide; p. 71-79.

Mazur P, Rall WF, Leibo SP. Kinetics of water loss and the likelihood of intracellular freezing in mouse ova. Influence of the method of calculating the temperature dependence of water permeability. Cell Biophys. 1984; 6:197–213. [PubMed: 6210147]

McGrath, JJ.; Gao, DY.; Tao, J.; Benson, C.; Critser, ES.; Critser, JK. Coupled transport across the murine oocyte plasma membrane: Water and cryoprotective agents. In: Toner, M.; Flik, MI.; Webb, DW.; Vader, DT.; Arimilli, RV.; Sauer, HJ.; Georgiadis, J.; Prasad, V., editors. Topics in heat transfer. New York: ASME Press; 1992. p. 1-14.

McGrath JJ, Fuller BJ, Hunter JE, Paynter S, Bernard AG. The permeability of fresh preovulatory human oocytes to dimethyl-sulfoxide at 3°C. CryoLetters. 1995; 16:79–84.

Mukherjee IN, Song YC, Sambanis A. Cryoprotectant delivery and removal from murine insulinomas at vitrification-relevant concentrations. Cryobiology. 2007; 55:10–18. [PubMed: 17533114]

Mullen SF, Li M, Li Y, Chen ZJ, Critser JK. Human oocyte vitrification: The permeability of metaphase II oocytes to water and ethylene glycol and the appliance toward vitrification. Fertil Steril. 2008; 89:1812–1825. [PubMed: 17681308]

Newton H, Pegg DE, Barrass R, Gosden RG. Osmotically inactive volume, hydraulic conductivity, and permeability to dimethyl sulphoxide of human mature oocytes. J Reprod Fertil. 1999; 117:27–33. [PubMed: 10645242]

Parkening TA, Tsunoda Y, Chang MC. Effects of various low temperatures, cryoprotective agents and cooling rates on the survival, fertilizability and development of frozen-thawed mouse eggs. J Exp Zool. 1976; 197:369–374. [PubMed: 965915]

Paynter SJ, Fuller BJ, Shaw RW. Temperature dependence of mature mouse oocyte membrane permeabilities in the presence of cryoprotectant. Cryobiology. 1997; 34:122–130. [PubMed: 9130385]

Paynter SJ, Cooper A, Gregory L, Fuller BJ, Shaw RW. Permeability characteristics of human oocytes in the presence of the cryoprotectant dimethylsulphoxide. Hum Reprod. 1999; 14:2338–2342. [PubMed: 10469706]

Paynter SJ, O'Neil L, Fuller BJ, Shaw RW. Membrane permeability of human oocytes in the presence of the cryoprotectant propane-1,2-diol. Fertil Steril. 2001; 75:532–538. [PubMed: 11239537]

Porcu E, Fabbri R, Seracchioli R, Ciotti PM, Magrini O, Flamigni C. Birth of a healthy female after intracytoplasmic sperm injection of cryopreserved human oocytes. Fertil Steril. 1997; 68:724–726. [PubMed: 9341619]

Quintans CJ, Donaldson MJ, Bertolino MV, Pasqualini RS. Birth of two babies using oocytes that were cryopreserved in a choline-based freezing medium. Hum Reprod. 2002; 17:3149–3152. [PubMed: 12456615]

Ruffing NA, Steponkus PL, Pitt RE, Parks JE. Osmometric behavior, hydraulic conductivity, and incidence of intracellular ice formation in bovine oocytes at different developmental stages. Cryobiology. 1993; 30:562–580. [PubMed: 8306705]

Rule GS, Law P, Kruuv J, Lepock JR. Water permeability of mammalian cells as a function of temperature in the presence of dimethylsulfoxide: Correlation with the state of the membrane lipids. J Cell Physiol. 1980; 103:407–416. [PubMed: 6249829]

Shaw JM, Trounson AO. Parthenogenetic activation of unfertilized mouse oocytes by exposure to 1,2-propanediol is influenced by temperature, oocyte age, and cumulus removal. Gamete Res. 1989; 24:269–279. [PubMed: 2599505]

Songsasen N, Ratterree MS, VandeVoort CA, Pegg DE, Leibo SP. Permeability characteristics and osmotic sensitivity of rhesus monkey (Macaca mulatta) oocytes. Hum Reprod. 2002a; 17:1875–1884. [PubMed: 12093854]

Songsasen N, Yu IJ, Ratterree MS, VandeVoort CA, Leibo SP. Effect of chilling on the organization of tubulin and chromosomes in rhesus monkey oocytes. Fertil Steril. 2002b; 77:818–825. [PubMed: 11937140]

Tucker MJ, Wright G, Morton PC, Massey JB. Birth after cryopreservation of immature oocytes with subsequent in vitro maturation. Fertil Steril. 1998; 70:578–579. [PubMed: 9757897]

Van den Abbeel E, Schneider U, Liu J, Agca Y, Critser JK, Van Steirteghem A. Osmotic responses and tolerance limits to changes in external osmolalities, and oolemma permeability characteristics, of human in vitro matured MII oocytes. Hum Reprod. 2007; 22:1959–1972. [PubMed: 17428880]

Van der Elst J, Van den Abbeel E, Nerinckx S, Van Steirteghem A. Parthenogenetic activation pattern and microtubular organization of the mouse oocyte after exposure to 1,2-propanediol. Cryobiology. 1992; 29:549–562. [PubMed: 1424712]

Vincent C, Johnson MH. Cooling, cryoprotectants, and the cytoskeleton of the mammalian oocyte. Oxf Rev Reprod Biol. 1992; 14:73–100. [PubMed: 1437216]

Whittingham DG. Fertilization in vitro and development to term of unfertilized mouse oocytes previously stored at −196°C. J Reprod Fertil. 1977; 49:89–94. [PubMed: 833794]

Yoon TK, Chung HM, Lim JM, Han SY, Ko JJ, Cha KY. Pregnancy and delivery of healthy infants developed from vitrified oocytes in a stimulated in vitro fertilization-embryo transfer program [letter]. Fertil Steril. 2000; 74:180–181. [PubMed: 10899519]

Younis AI, Toner M, Albertini DF, Biggers JD. Cryobiology of non-human primate oocytes. Hum Reprod. 1996; 11:156–165. [PubMed: 8671179]

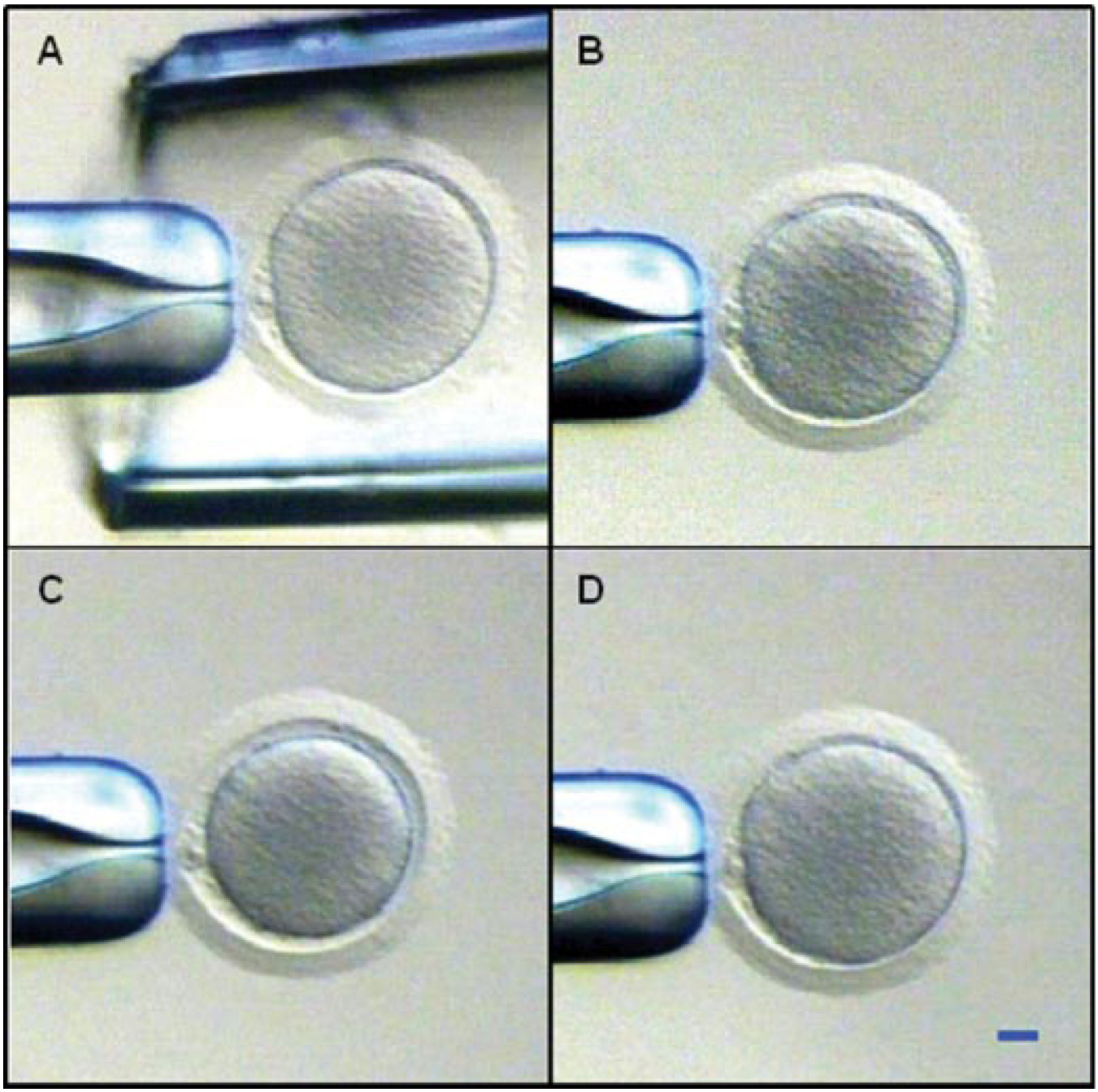

Figure 1.

Typical shrink-and-swell response of a mature rhesus monkey oocyte during exposure to a penetrating cryoprotectant additive. **A**: Oocyte held in isotonic medium within the tip of an outer pipette, just prior to cryoprotectant exposure. Subsequent images show the same oocyte after exposure to a 1.1 M solution of ethylene glycol for 5 sec (**B**), 1 min (**C**), and 16 min (**D**). Scale bar represents 20 μm. [See color version online at www.interscience.wiley.com.]

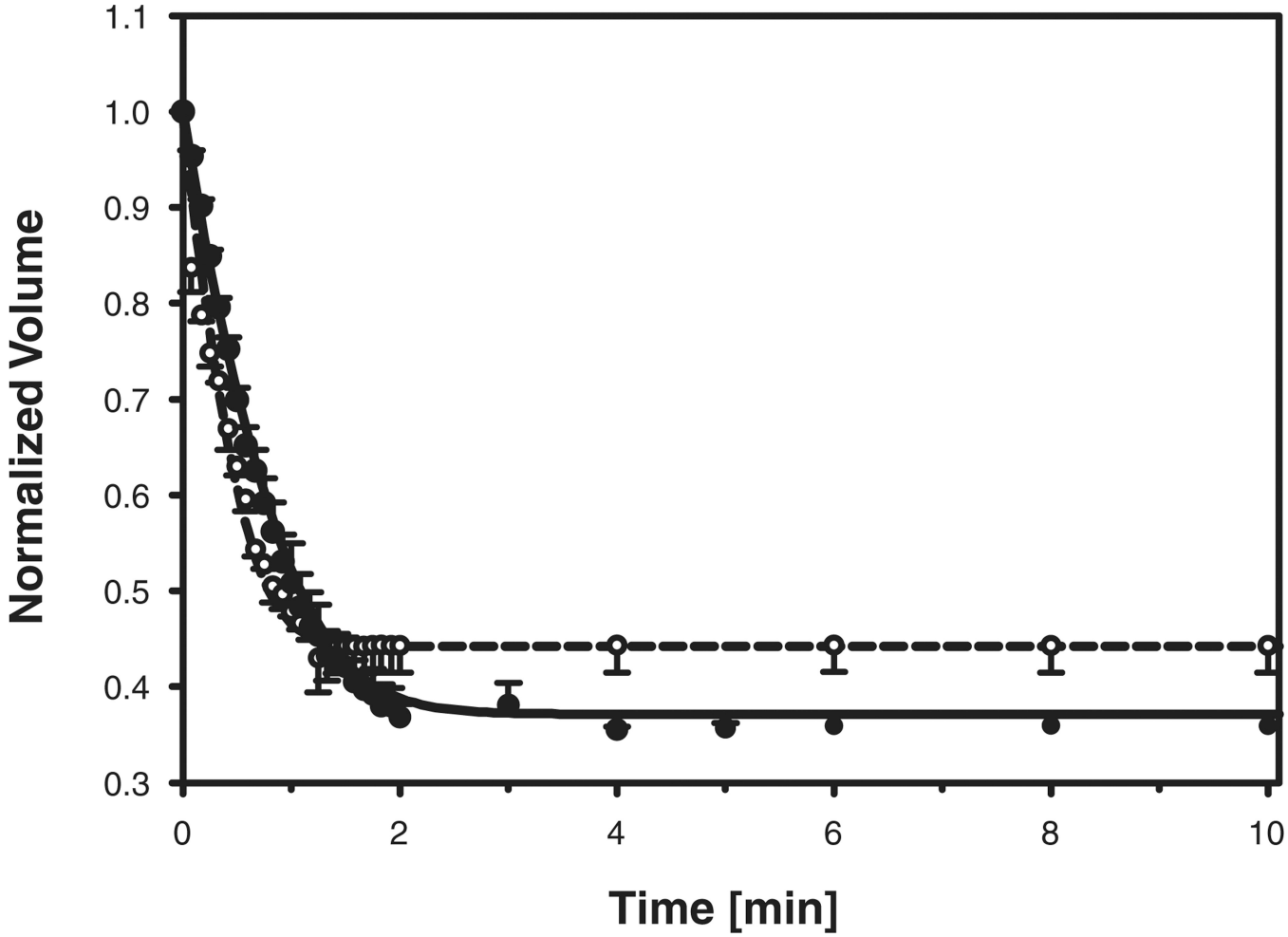

Figure 2.

Volume of mature (closed symbols; solid line) and immature (open symbols; dashed line) rhesus monkey oocytes, normalized to the isotonic cell volume, as a function of time exposed to hypertonic PBS. Symbols and error bars represent the average and standard error, respectively, of the normalized volumes measured at each timepoint. Whereas the data are from experiments with four mature and two immature oocytes, measurements could not always be made at each timepoint, resulting in missing values; the number of measurements averaged at each time-point is indicated by the size of the corresponding circular symbol (the smallest symbols represent n=1, and the largest represent n=4). The solid and dashed curves represent model predictions for mature and immature oocytes, respectively, using averaged values of the hydraulic conductivity (see Table 1) and osmotically inactive volume fraction (see text).

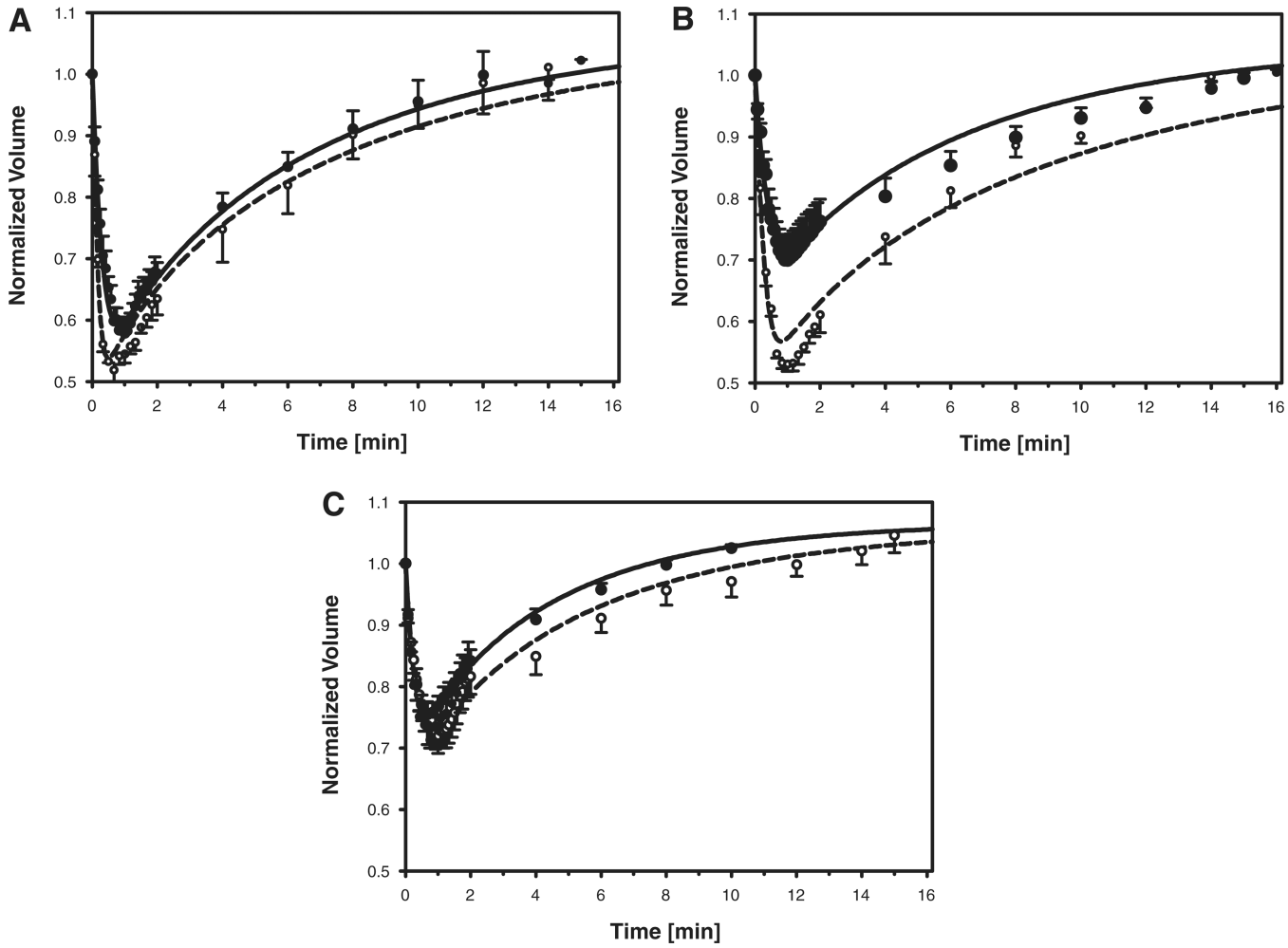

Figure 3.

Volume of mature (closed symbols; solid line) and immature (open symbols; dashed line) rhesus monkey oocytes, normalized to the isotonic cell volume, as a function of time exposed to DMSO (**A**), EG (**B**), or PROH (**C**). Symbols and error bars represent the average and standard error, respectively, of the normalized volumes measured at each timepoint. Whereas the data are from experiments with four to seven mature oocytes and two to four immature oocytes, measurements could not always be made at each timepoint, resulting in missing values; the number of measurements averaged at each timepoint is indicated by the size of the corresponding circular symbol (the smallest symbols represent n=2, and the largest represent n=7). The solid and dashed curves represent model predictions for mature and immature oocytes, respectively, using averaged values of the membrane permeability parameters (see Table 1) and osmotically inactive volume fraction (see text).

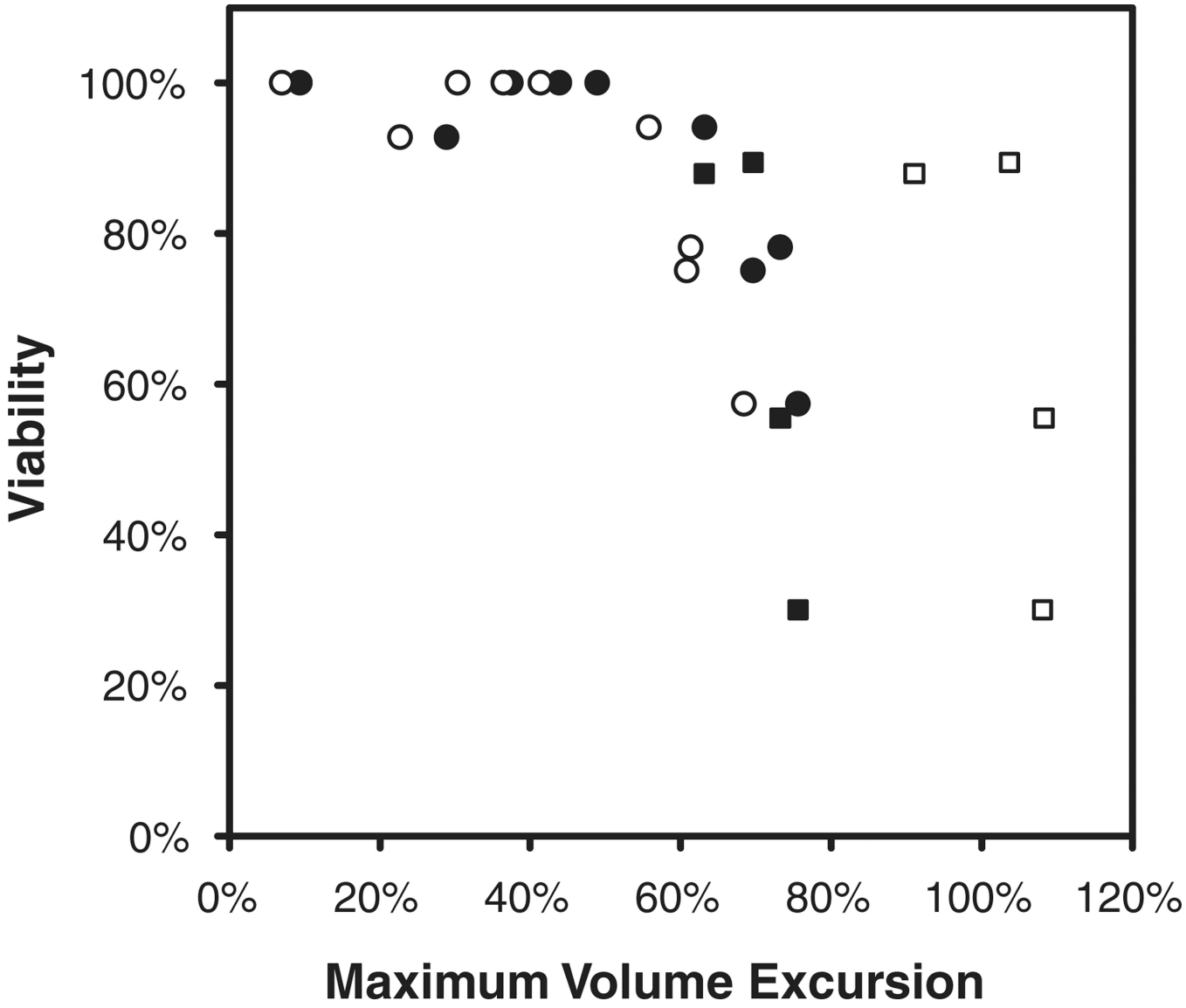

Figure 4.

Correlation of rhesus oocyte viability with the predicted maximum volume excursion during exposure to 0.1–5.0 M EG for 5 (circles) or 10 min (squares), followed by abrupt dilution in isotonic media. Viability data and oocyte permeability characteristics are adapted from Songsasen et al. (2002a). Closed symbols represent the predicted maximum volume reduction during EG addition, and open symbols indicate the predicted maximum volume increase during the subsequent dilution step.

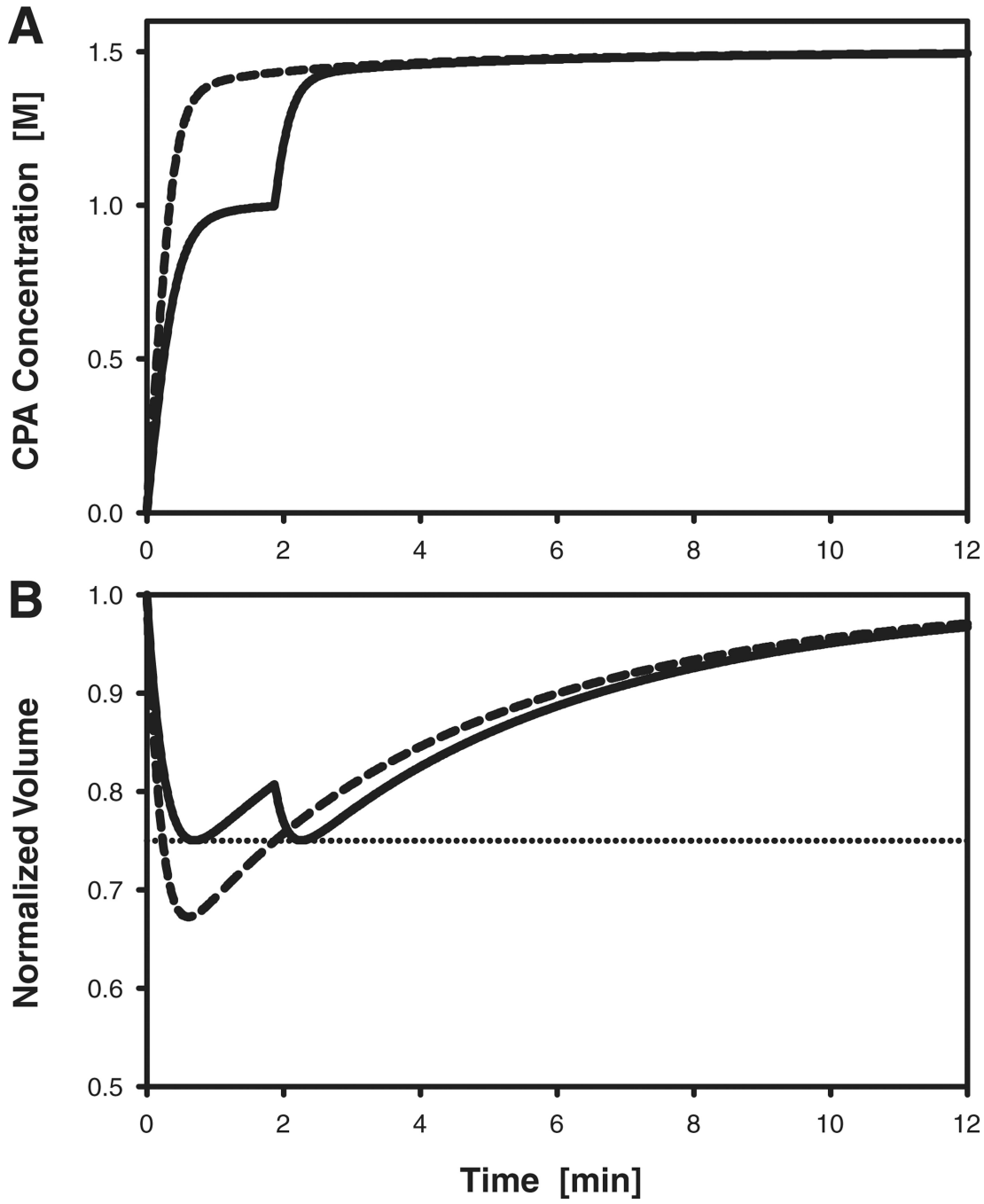

Figure 5.

Predicted response of rhesus monkey oocytes during addition of PROH to achieve a final intracellular concentration of 1.5 M. **A**: Intracellular concentration of PROH. **B**: Oocyte volume, normalized to the isotonic cell volume; the horizontal dotted line indicates the lower bound of the assumed range of tolerable volume excursions (75–125% of the isotonic volume). Dashed curves represent the response to a nonoptimized single-step CPA addition process, in which oocytes are transferred directly to a solution containing 1.5 M PROH. Solid curves represent the response to an optimized two-step addition process, in which

oocytes are first exposed to a solution containing 1M PROH for 1.9 min before transfer to the 1.5 M PROH solution.

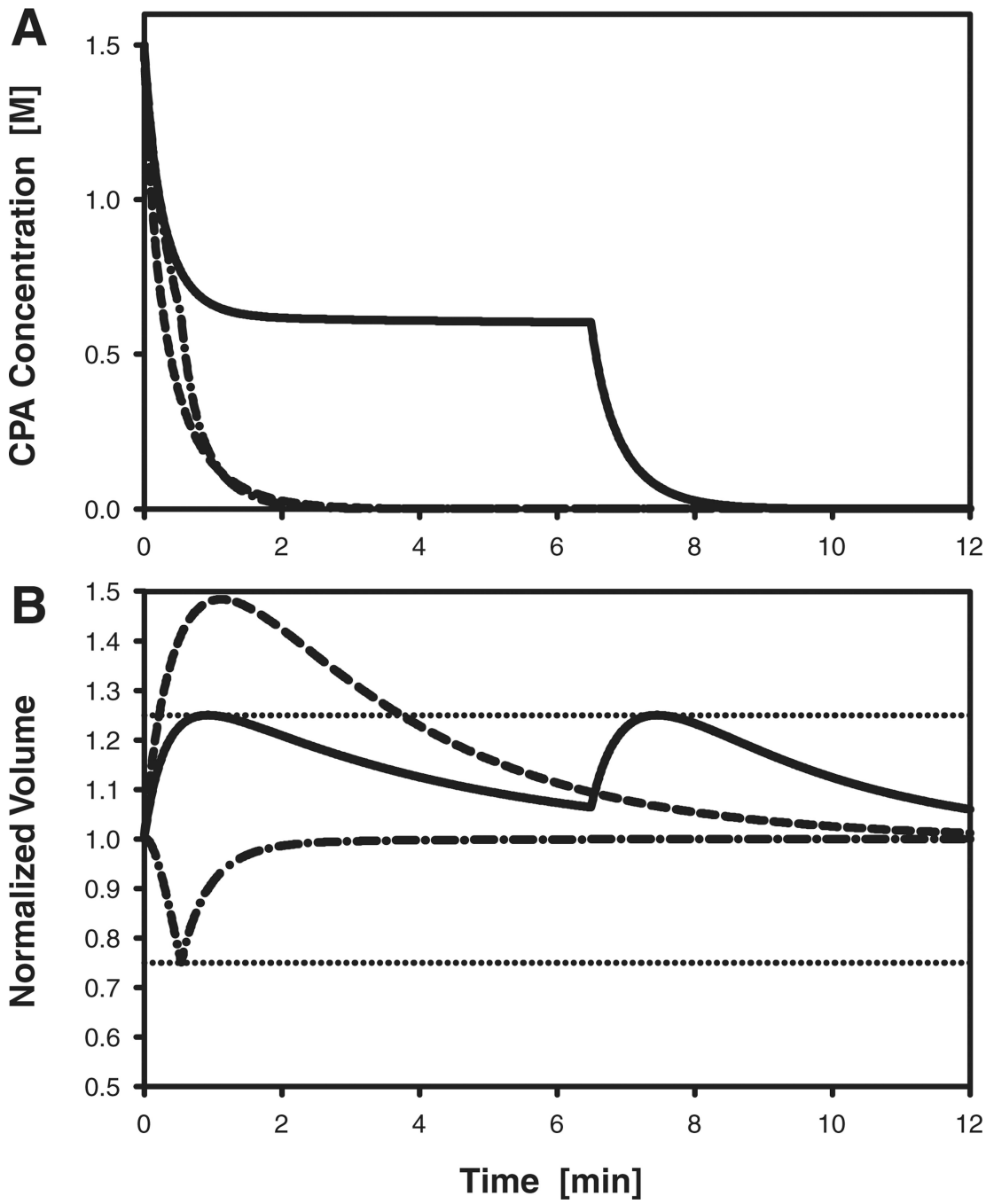

Figure 6.

Predicted response of rhesus monkey oocytes during dilution of PROH, which is initially present at an intracellular concentration of 1.5 M. **A**: Intracellular concentration of PROH. **B**: Oocyte volume, normalized to the isotonic cell volume; the horizontal dotted lines indicate the upper and lower bounds of the assumed range of tolerable volume excursions (75–125% of the isotonic volume). Dashed curves represent the response to a nonoptimized single-step dilution process, in which oocytes are transferred directly to isotonic medium. Solid curves represent the response to an optimized two-step dilution process, in which

oocytes are first exposed to a solution containing 0.6 M PROH for 6.5 min before transfer to isotonic medium. Dash-dotted curves represent the response to an optimized two-step dilution method that uses sucrose as an osmotic buffer: oocytes are first exposed to a solution containing 1Msucrose for 32 sec before transfer to isotonic medium.

TABLE 1

Hydraulic Conductivity (L_p) and Solute Permeability (P_s) of Rhesus Monkey Oocyte Membrane at Room Temperature (23.5°C)

	L_p (μm/min/atm)		P_s (μm/sec)	
Solution	**Immature***	**Mature†**	**Immature***	**Mature†**
Hypertonic PBS	$0.81 \pm 0.01^{b,c}$	0.55 ± 0.05^{c}	—	—
DMSO	1.68 ± 0.23^{a}	1.01 ± 0.10^{b}	0.15 ± 0.03^{e}	0.24 ± 0.02^{e}
EG	$1.00 \pm 0.11^{b,c}$	0.61 ± 0.07^{c}	0.12 ± 0.02^{e}	$0.34 \pm 0.07^{d,e}$
PROH	$0.72 \pm 0.13^{b,c}$	$0.86 \pm 0.06^{b,c}$	$0.31 \pm 0.06^{d,e}$	0.56 ± 0.05^{d}

Shown are the average and standard error of the best-fit parameters for 2–4 immature oocytes or 4–7 mature oocytes; distinct superscript letters (a–e) indicate statistically significant differences ($P < 0.05$; Tukey's HSD test).

* GV or GVBD stage.

† M II stage.